

Cramér-Rao Bound Based Waveform Optimization for MIMO Radar: An Efficient Linear-Proximal Method

Xiaohua Zhou*, Xu Du[†], Yijie Mao*

*School of Information Science and Technology, ShanghaiTech University, Shanghai 201210, China

[†]Institute of Mathematics HNAS, Henan Academy of Science, Zhengzhou 450000, China

Email:{zhouxh3, maoyj}@shanghaitech.edu.cn, duxu@hnas.ac.cn

Abstract—This paper focuses on radar waveform optimization for minimizing the Cramér-Rao bound (CRB) in a multiple-input multiple-output (MIMO) radar system. In contrast to conventional approaches relying on semi-definite programming (SDP) and optimization toolboxes like CVX, we introduce a pioneering and efficient waveform optimization approach in this paper. Our proposed algorithm first applies sequential linear approximation to transform the original CRB-based problem with the transmit power constraint into a sequence of convex subproblems. By introducing a proximal term and further leveraging the Karush-Kuhn-Tucker (KKT) conditions, we derive the optimal closed-form solution for each subproblem. The convergence of the proposed algorithm is then proved rigorously. Numerical results demonstrate that the proposed approach significantly reduces computational complexity — at least two orders of magnitude lower than the baseline algorithms while maintaining the same radar sensing accuracy.

Index Terms—Cramér-Rao bound (CRB), radar sensing, target detection, waveform design.

I. INTRODUCTION

Nowadays, positioning and sensing have received considerable attention as key enablers for a series of emerging applications such as augmented reality, virtual reality, the internet of things, autonomous driving, and space-air-ground integrated networks, which simultaneously require high data rate communications and accurate positioning and sensing [1]. In this context, radar plays a crucial role by offering advanced capabilities for accurate target detection, localization, and tracking. Multiple-input multiple-output (MIMO) radar, in particular, is favored for its superior performance compared to traditional radar systems. It is highly valuable in applications like defense, surveillance, and remote sensing [2], [3]. The study of waveform design in the context of MIMO radar has been extensively explored with the aim of improving estimation accuracy [4]. Radar waveform design can be classified into the following four categories [2]: 1) design waveforms based on information theoretic measures, minimum

mean-square error estimation (MMSE), or Cramér-Rao bound (CRB), 2) design waveforms with good auto/cross-correlation properties, 3) design desired transmit beam patterns, and 4) jointly design the transmit waveforms and receive filters for enhancing target detection performance. This paper primarily focuses on the first category, specifically the CRB-based waveform design, which has been widely applied in integrated sensing and communication (ISAC) [5], [6], localization [7], and underwater acoustic sensor networks (UASNs) [8], etc.

CRB, a lower bound on the variance of unbiased estimators, is equivalent to the inverse of the Fisher information matrix (FIM). Since optimizing a matrix as an objective function is impossible, several scalar mapping of FIM has been studied in existing works [9], [10], and [11, Chapter 7.5.2] including: a) the trace of the inverse of FIM, b) the maximum eigenvalue of the inverse of FIM, c) the determinant of the inverse of FIM, d) the maximal diagonal element of the inverse of FIM. Readers are referred to [10] for a detailed summary for all mapping criteria. For solving the optimization problems with the aforementioned scalar mappings of FIM, several optimization algorithms have been developed [5], [9], [12]. These algorithms all share the common approach of approximating the original problem into a semi-definite programming (SDP) by lifting the beamforming vector variable into positive semi-definite matrix variable [13]–[15] and relaxing the rank-one constraint. After solving the SDP based on the solvers in optimization toolboxes such as CVX [16], post processing is carried out to recover the *vector space precoder* based on eigenvalue decomposition (EVD) [5], [12] or Gaussian randomization [17], [18]. These approaches, also known as semi-definite relaxation (SDR) [14], [19]–[21], come with significant drawbacks that must be acknowledged. First, employing standard solvers in optimization toolboxes to solve SDP often results in high computational complexity, making it impractical for practical applications. Second, the post processing methods based on EVD or Gaussian randomization are susceptible to numerical instability, potentially resulting in the failure to meet the rank-one constraint. They are also lack of theoretical guarantees to ensure the optimality conditions. Third, there are relatively few studies on efficiently solving

This work has been supported in part by the National Nature Science Foundation of China under Grant 62201347; in part by Shanghai Sailing Program under Grant 22YF1428400; and in part High-level Talent Research Start-up Project Funding of Henan Academy of Sciences (Project NO.241819034). (Corresponding author: Yijie Mao)

SDPs, especially for non-convex SDPs. Therefore, there is an urgent need for efficient algorithms that can directly derive the solution of the beamforming vectors without relying on SDR and optimization toolboxes. Unfortunately, to the best of our knowledge, such an approach has yet to be uncovered in existing literature.

This paper aims at closing this gap by proposing an efficient waveform optimization algorithm for the CRB-based radar sensing problems. Inspired by our recent work [22], we propose an iterative algorithm which employs linear approximation techniques for the objective function and the sequential quadratic programming (SQP) theory [23] for the transmit power constraint. Additionally, we introduce an L_2 norm proximal term [24], [25] to ensure the convexity of the augmented objective function.

Contributions of this paper are summarized as follows:

- A novel optimization algorithm is proposed to tackle the CRB-based waveform design problem with a transmit power constraint. Specifically, we propose an iterative algorithm by solving a sequence of approximated convex subproblems. A closed-form solution is obtained for each subproblem, which therefore eliminates the need for optimization toolbox. Moreover, the proposed algorithm derives the beamforming vectors' solution directly without the need for SDR.
- The sub-linear convergence property [26, Thm 2.1.14] of the proposed algorithm is then proved rigorously.
- Numerical results are conducted to demonstrate that the proposed algorithm significantly reduces CPU time by at least two orders of magnitude compared to traditional methods while maintaining comparable radar sensing performance.

Organizations: The rest of the following paper is structured as follows. Section II presents the system model. Section III discusses problem formulation and the existing algorithms. In Section IV, we introduce the proposed *Linear-Proximal Method* to solve the non-convex SDP problem. Section V presents the simulation results, followed by conclusion in Section VI.

Notations: Bold upper and lower case letters denote matrices and column vectors, respectively. $\Re(\cdot)$ and $\Im(\cdot)$ respectively denote the real and imaginary parts of a complex scalar, vector, or matrix. $(\cdot)^\top$, $(\cdot)^H$, $|\cdot|$, $\|\cdot\|$, $(\cdot)^{-1}$, and $\text{tr}(\cdot)$ represent the transpose, Hermitian, absolute value, Euclidean norm, inverse, and trace operators, respectively.

II. SYSTEM MODEL

We consider a monostatic radar system equipped with N_t transmit antennas and N_r receive antennas, aiming to detect the position of a single target¹. There are L transmission and radar pulse blocks in one coherent processing interval (CPI) indexed by $\mathcal{L} = \{1, \dots, L\}$. The overall transmit signal from

¹For simplified illustration, we consider a single target in this work. However, the proposed algorithm can be easily extended to a multi-target scenario.

the MIMO radar is $\mathbf{X} = [\mathbf{x}[1], \mathbf{x}[2], \dots, \mathbf{x}[L]] \in \mathbb{C}^{N_t \times L}$. In each transmission block l , this MIMO radar receives the following reflected echo from the target:

$$\mathbf{y}_r[l] = \beta e^{j2\pi\mathcal{F}_D l T} \mathbf{a}_r(\theta) \mathbf{a}_t^H(\theta) \mathbf{x}[l] + \mathbf{z}_r[l], \quad (1)$$

where β represents the reflection coefficient, measuring the portion of the incident electromagnetic wave reflected back to the MIMO radar. \mathcal{F}_D represents the Doppler frequency. It is calculated by $\mathcal{F}_D = \frac{2v f_c}{c}$, where v is the velocity of the target, f_c is the carrier frequency, and c denotes the speed of light. $\mathbf{z}_r[l] \in \mathbb{C}^{N_r \times 1}$ is an additive white Gaussian noise vector with each element having a zero mean and a variance of σ_r^2 . $\mathbf{a}_t(\theta) \in \mathbb{C}^{N_t \times 1}$ and $\mathbf{a}_r(\theta) \in \mathbb{C}^{N_r \times 1}$ respectively represent the steering vectors for the transmit and receive antenna array, which are defined as:

$$\mathbf{a}_t(\theta) = [1, e^{j\pi \sin(\theta)}, \dots, e^{j\pi(N_t-1) \sin(\theta)}],$$

$$\mathbf{a}_r(\theta) = [1, e^{j\pi \sin(\theta)}, \dots, e^{j\pi(N_r-1) \sin(\theta)}],$$

where θ denotes the angle of departure and arrival for the line of sight (LoS) path of the monostatic radar.

The covariance of the transmit signal is denoted as:

$$\mathbf{P} \stackrel{\text{def}}{=} \frac{1}{L} \sum_{l=1}^L \mathbf{x}[l] \mathbf{x}[l]^H = \mathbf{p} \mathbf{p}^H, \quad (2)$$

where $\mathbf{p} \in \mathbb{C}^{N_t \times 1}$ is the beamforming vector of the transmit signal.

Define the vector for estimation parameters as $\boldsymbol{\xi} = [\theta, \beta^{\Re}, \beta^{\Im}, \mathcal{F}_D]^T$, where θ is the direction of departure (DoD) and direction of arrival (DoA) of the target, β^{\Re} denotes the real part of the complex coefficient, β^{\Im} represents the imaginary part of the complex coefficient, and \mathcal{F}_D is the doppler frequency. The FIM matrix used to estimate all parameters in $\boldsymbol{\xi}$ is given as [5]:

$$\mathbf{F}(\mathbf{p}) = \begin{bmatrix} F_{11} & F_{12} & F_{13} & F_{14} \\ F_{21} & F_{22} & F_{23} & F_{24} \\ F_{31} & F_{32} & F_{33} & F_{34} \\ F_{41} & F_{42} & F_{43} & F_{44} \end{bmatrix}, \quad (3)$$

where the elements of FIM are evaluated as

$$F_{ij} = \frac{2}{\sigma_r^2} \Re \left\{ \sum_{l=1}^L \frac{\partial \boldsymbol{\mu}^\top[l]}{\partial \boldsymbol{\xi}_i} \frac{\partial \boldsymbol{\mu}[l]}{\partial \boldsymbol{\xi}_j} \right\}, \forall i, j = 1, \dots, 4, \quad (4)$$

where $\boldsymbol{\xi}_i$, $\boldsymbol{\xi}_j$ are the i th and the j th elements of $\boldsymbol{\xi}$, and $\boldsymbol{\mu}[l] = \mathbf{y}_r[l] - \mathbf{z}_r[l]$.

III. PROBLEM FORMULATION AND EXISTING ALGORITHMS

Based on the FIM matrix defined in (3), we then obtain the CRB metric as \mathbf{F}^{-1} . There are two classical transmit beamforming optimization problems based on CRB: minimizing the trace of inverse of FIM [4] and minimizing the largest eigenvalue of the inverse of FIM [5], both subject to the transmit power constraint.

The optimization problem based on minimizing the trace of inverse of FIM is formulated as:

$$\begin{aligned} \min_{\mathbf{P}} \quad & \text{tr}(\mathbf{F}^{-1}) \\ \text{s. t.} \quad & \text{tr}(\mathbf{p}\mathbf{p}^H) \leq P_t. \end{aligned} \quad (5)$$

To circumvent the need for inversion in Problem (5), existing works typically utilize the Schur complement to reformulate the problem as [12]:

$$\begin{aligned} \min_{\mathbf{P}, t_1, t_2, t_3, t_4} \quad & \sum_{i=1}^4 t_i \\ \text{s. t.} \quad & \begin{bmatrix} \mathbf{F} & \mathbf{e}_i \\ \mathbf{e}_i^T & t_i \end{bmatrix} \succeq 0, i \in \{1, 2, 3, 4\}, \\ & \text{tr}(\mathbf{P}) \leq P_t, \\ & \text{rank}(\mathbf{P}) = 1, \end{aligned} \quad (6)$$

where t_1, \dots, t_4 are auxiliary variables, and \mathbf{e}_i is the i -column of a 4×4 identity matrix.

The optimization problem based on minimizing the largest eigenvalue of FIM is given as:

$$\begin{aligned} \min_{\mathbf{P}} \quad & \sigma_{\max}(\mathbf{F}^{-1}) \\ \text{s. t.} \quad & \text{tr}(\mathbf{p}\mathbf{p}^H) \leq P_t. \end{aligned} \quad (7)$$

By introducing an auxiliary variable t , Problem (7) can be equivalently reformulated as [14]:

$$\begin{aligned} \max_{\mathbf{P}, t} \quad & t \\ \text{s. t.} \quad & \mathbf{F} \succeq t\mathbf{I}, \\ & \text{tr}(\mathbf{P}) \leq P_t, \\ & \text{rank}(\mathbf{P}) = 1. \end{aligned} \quad (8)$$

Since Problem (5) minimizes the sum of all eigenvalues of the inverse of FIM, while Problem (7) only minimizes the maximum eigenvalue of the inverse of FIM, the CRB performance obtained by solving Problem (5) is always better than the one obtained from solving Problem (7). Therefore, Problem (5) is preferred in most literature [9], [12], [27]. This paper focuses on addressing Problem (5) efficiently.

For Problem (5), the reformulated problem (6) is a convex SDP if removing the rank-one constraint. Therefore, the optimal covariance matrix \mathbf{P} for the relaxed problem without the rank-one constraint can be directly obtained by the standard optimization toolbox like CVX [16]. Such approach is known as SDR. However, removing the rank-one constraint in (6) may lead to a solution \mathbf{P} that is not rank-one. Although the transmit beamforming solution \mathbf{p} can be restored through EVD [5] or Gaussian randomization [18], the solution might not be optimal for the original non-convex problem. Furthermore, solving SDP via CVX toolbox essentially employs interior-point methods, which are known for their high computational complexity.

In this paper, the following strategies are demonstrated as the baselines. For later convenience, we abbreviate them as follows: a) *SDP-EVD* for the method of using SDR and EVD to solve Problem (6); b) *SDP-random* for the approach that solves Problem (6) by SDR combined with Gaussian randomization;

c) *Upper-Bound* for the approach which removes the rank-one constraint in (6), and solves the corresponding relaxed convex problem using the standard optimization toolbox CVX. The aforementioned first two baselines are summarized in Algorithm 1. The third baseline is obtained by simply removing step 2 of Algorithm 1.

Algorithm 1: Baseline 1-2

Input: $\theta, \beta^{\Re}, \beta^{\Im}, \mathcal{F}_D$;

- 1: Update \mathbf{P} by removing the rank-one constraint in Problem (6) and solving the corresponding relaxed problem via CVX toolbox;
- 2: Calculate \mathbf{p} through EVD/Gaussian randomization.

Output: \mathbf{p} ;

IV. PROPOSED ALGORITHM

In this section, to circumvent the reliance on optimization toolboxes and address the issue of matrix inversion in (5), we propose a novel algorithm named *Linear-Proximal Method* (LPM), which iteratively solves a sequence of convex subproblems. In the end, we provide the corresponding convergence analysis.

A. Linear-Proximal Method

In order to deal with the symbolic inverse of FIM in the objective function of (5) while avoiding the matrix inequalities and matrix variables as in (6), inspired from [22, Equation 9], we adopt a tight linearized approximation of $\text{tr}(\mathbf{F}^{-1})$ to approximate Problem (5) into a sequence of subproblems. The subproblem in the $(k+1)$ -th iteration is:

$$\begin{aligned} \min_{\mathbf{P}} \quad & \text{tr}((\mathbf{F}^k)^{-1}) - \text{tr}((\mathbf{F}^k)^{-1} \mathbf{F} (\mathbf{F}^k)^{-1}) \\ \text{s. t.} \quad & \text{tr}(\mathbf{p}\mathbf{p}^H) \leq P_t, \end{aligned} \quad (9)$$

where \mathbf{F}^k represents the numerical value matrix of \mathbf{F} derived based on the solution \mathbf{p}^k in the (k) -th iteration.

Following the standard SQP theory [23, Chapter 18], linearization is applied to the transmit power constraint of (9), which approximates the quadratic term $\text{tr}(\mathbf{p}\mathbf{p}^H)$ to $\text{tr}(\mathbf{p}^k(\mathbf{p}^k)^H) + 2(\mathbf{p}^k)^H(\mathbf{p} - \mathbf{p}^k)$ with the solution of \mathbf{p}^k obtained from the (k) -th iteration. This linearization also adds the term $\lambda^k \mathbf{p}^H \mathbf{p}$ to the objective function guaranteeing that the KKT conditions are satisfied, where λ^k denotes the value of the dual variable λ introduced by the transmit power constraint in Problem (9) during the (k) -th iteration. Problem (9) is then equivalently transformed to:

$$\begin{aligned} \min_{\mathbf{P}} \quad & \lambda^k \mathbf{p}^H \mathbf{p} - \text{tr}((\mathbf{F}^k)^{-1} \mathbf{F} (\mathbf{F}^k)^{-1}) \\ \text{s. t.} \quad & \text{tr}(\mathbf{p}^k(\mathbf{p}^k)^H) + 2(\mathbf{p}^k)^H(\mathbf{p} - \mathbf{p}^k) = P_t | \lambda. \end{aligned} \quad (10)$$

Unfortunately, the objective function of Problem (10) remains non-convex. To address the issue, we introduce an L_2 -norm proximal term in the objective function. Moreover, the term $\text{tr}((\mathbf{F}^k)^{-1} \mathbf{F} (\mathbf{F}^k)^{-1})$ is also equivalently transformed to $\sum_{i=1}^4 \sum_{j=1}^4 a_{ij} F_{ji}$, where $a_{ij}, \forall i, j \in \{1, \dots, 4\}$ denote

the elements of $(\mathbf{F}^k)^{-1}(\mathbf{F}^k)^{-1}$, and $F_{ji}, \forall i, j = 1, \dots, 4$ are defined in (4). The resulting problem becomes:

$$\begin{aligned} \min_{\mathbf{p}} \quad & -\sum_{i=1}^4 \sum_{j=1}^4 a_{ij} F_{ji} + \lambda^k \mathbf{p}^H \mathbf{p} + \frac{\rho}{2} \|\mathbf{p} - \mathbf{p}^k\|^2 \\ \text{s. t.} \quad & \text{tr}(\mathbf{p}^k (\mathbf{p}^k)^H) + 2(\mathbf{p}^k)^H (\mathbf{p} - \mathbf{p}^k) = P_t \mid \lambda, \end{aligned} \quad (11)$$

where $\rho > 0$ is a sufficient penalty coefficient. With a sufficient large ρ , the proximal term $\frac{\rho}{2} \|\mathbf{p} - \mathbf{p}^k\|^2$ ensures the convexity of the objective function, thereby facilitating stable numerical convergence of the algorithm.

Note that, the Lagrange function of the convex Problem (11) is obtained as follows:

$$\begin{aligned} \mathcal{L}(\mathbf{p}, \lambda) = & -\sum_{i=1}^4 \sum_{j=1}^4 a_{ij} F_{ji} + \lambda^k \mathbf{p}^H \mathbf{p} + \frac{\rho}{2} \|\mathbf{p} - \mathbf{p}^k\|^2 \\ & + \lambda \left[\text{tr}(\mathbf{p}^k (\mathbf{p}^k)^H) + 2(\mathbf{p}^k)^H (\mathbf{p} - \mathbf{p}^k) - P_t \right], \end{aligned}$$

while the corresponding Karush-Kuhn-Tucker (KKT) stationary condition is expressed as:

$$\begin{cases} \frac{\partial \mathcal{L}}{\partial \mathbf{p}} = \mathbf{Q}^k \mathbf{p} + 2\lambda \mathbf{p}^k - \rho \mathbf{p}^k = \mathbf{0} \\ \frac{\partial \mathcal{L}}{\partial \lambda} = \text{tr}(\mathbf{p}^k (\mathbf{p}^k)^H) + 2(\mathbf{p}^k)^H (\mathbf{p} - \mathbf{p}^k) - P_t = 0, \end{cases} \quad (12)$$

where $\mathbf{Q}^k = -\frac{1}{\sigma_r^2} \boldsymbol{\Theta} + 2\lambda^k \mathbf{I} + \rho \mathbf{I}$, \mathbf{I} denotes the identity matrix, and $\boldsymbol{\Theta}$ is given as

$$\begin{aligned} \boldsymbol{\Theta} = & b \left(\frac{\partial \mathbf{A}(\theta)}{\partial \theta} \right)^H \frac{\partial \mathbf{A}(\theta)}{\partial \theta} + c \mathbf{A}^H(\theta) \frac{\partial \mathbf{A}(\theta)}{\partial \theta} \\ & + d \left(\frac{\partial \mathbf{A}(\theta)}{\partial \theta} \right)^H \mathbf{A}(\theta) + e \mathbf{A}^H(\theta) \mathbf{A}(\theta). \end{aligned}$$

Here, $\mathbf{A}(\theta) = \mathbf{a}_r(\theta) \mathbf{a}_t^H(\theta)$. b, c, d, e in $\boldsymbol{\Theta}$ are given as:

$$\begin{aligned} b = & 2L|\beta|^2 a_{11}, \\ c = & L\beta a_{21} - L\beta a_{31}j - \pi(L+1)|\beta|^2 a_{41}j + L\beta a_{12} \\ & - L\beta a_{13}j - \pi(L+1)|\beta|^2 a_{14}j, \\ d = & L\beta^* a_{21} + L\beta^* a_{31}j + \pi(L+1)|\beta|^2 a_{41}j + L\beta^* a_{12} \\ & + L\beta^* a_{13}j + \pi(L+1)|\beta|^2 a_{14}j, \\ e = & 2La_{22} + \pi(L+1)(\beta - \beta^*)a_{42}j + \pi(L+1)(\beta + \beta^*)a_{43} \\ & + \pi(L+1)(\beta - \beta^*)a_{24}j + \pi(L+1)(\beta + \beta^*)a_{34} \\ & + 2La_{33} + \left(\frac{4\pi^2}{L} \right) \frac{(L+1)(2L+1)}{3} |\beta|^2 a_{44}. \end{aligned}$$

By solving Equation (12), the optimal dual and primal variables are obtained as:

$$\lambda^* = \frac{\rho}{2} - \frac{P_t + (\mathbf{p}^k)^H \mathbf{p}^k}{4(\mathbf{p}^k)^H (\mathbf{Q}^k)^{-1} \mathbf{p}^k}, \quad (13a)$$

$$\mathbf{p}^* = (\rho - 2\lambda^{k+1})(\mathbf{Q}^k)^{-1} \mathbf{p}^k. \quad (13b)$$

We then update λ^{k+1} and \mathbf{p}^{k+1} using (13). The details of the proposed LPM is illustrated in Algorithm 2. Specifically, the dual variable λ and the beamforming vector \mathbf{p} are iteratively updated until the convergence of the objective function obj^k of Problem (9), ϵ is the convergence tolerance.

Algorithm 2: Linear-Proximal Method (LPM)

Input: $\theta, \beta^{\Re}, \beta^{\Im}, \mathcal{F}_D$;

1: **Initialization:** Initialize feasible \mathbf{p}^0 and \mathbf{F}^0 , initial iteration index $k \leftarrow 0$ and tolerance $\epsilon > 0$;

2: **repeat**

3: Update λ^{k+1} by Equation (13a);

4: Update \mathbf{p}^{k+1} by Equation (13b);

5: Evaluate the objective function obj^{k+1} in Problem (9);

6: **until** $|obj^{k+1} - obj^k| \leq \epsilon$;

7: Set $\mathbf{p}^* \leftarrow \mathbf{p}^{k+1}$;

8: **return** \mathbf{p}^* .

Output: \mathbf{p}^* ;

B. Convergence Analysis and Computational Complexity

1) *Convergence Analysis:* Next, we analyze the convergence of Algorithm 2. In the following, we assume that \mathbf{p}^0 is initialized in the neighborhood of a local optimal solution \mathbf{p}^* . We can then show the sub-linear convergence of Algorithm 2 by checking the limit of the following equation:

$$\frac{\|\mathbf{p}^{k+1} - \mathbf{p}^*\|}{\|\mathbf{p}^k - \mathbf{p}^*\|} \stackrel{(13b)}{=} \frac{\|(\rho - 2\lambda^{k+1})(\mathbf{Q}^k)^{-1} \mathbf{p}^k - \mathbf{p}^*\|}{\|\mathbf{p}^k - \mathbf{p}^*\|}. \quad (14)$$

As k approaches infinity, the coefficient of \mathbf{p}^k in the numerator of (14) shows:

$$\begin{aligned} & \lim_{k \rightarrow \infty} (\rho - 2\lambda^{k+1})(\mathbf{Q}^k)^{-1} \\ \stackrel{(13a)}{=} & \lim_{k \rightarrow \infty} \frac{1}{2} ((\mathbf{p}^k)^H (\mathbf{Q}^k)^{-1} \mathbf{p}^k)^{-1} (P_t + (\mathbf{p}^k)^H \mathbf{p}^k) (\mathbf{Q}^k)^{-1} \\ = & \lim_{k \rightarrow \infty} \frac{((\mathbf{p}^k)^H \mathbf{p}^k (\mathbf{Q}^k)^{-1})}{\|\mathbf{p}^k\|_{(\mathbf{Q}^k)^{-1}}^2} = \mathbf{I}, \end{aligned} \quad (15)$$

where $\|\cdot\|_{\mathbf{M}}$ denotes the Mahalanobis distance with symmetric positive definite matrix \mathbf{M} and it simplifies to the L_2 norm when $\mathbf{M} = \mathbf{I}$. The last equality results from the proximity of eigenvalues of matrix \mathbf{Q} caused by parameter ρ as well as the initial point \mathbf{p}^0 . Based on (14) and (15), we then obtain the sub-linear convergence property of Algorithm 2 by showing:

$$\lim_{k \rightarrow \infty} \frac{\|\mathbf{p}^{k+1} - \mathbf{p}^*\|}{\|\mathbf{p}^k - \mathbf{p}^*\|} = 1. \quad (16)$$

2) *Computational Complexity:* The complexities of both Algorithm 1 and Algorithm 2 are summarized here. In Algorithm 1, the SDP problem is solved using interior point methods by CVX, incurring a computational complexity of $\mathcal{O}(\log(N_t^7))$ [12], [28]. In Algorithm 2, each iteration for obtaining the closed-form solution \mathbf{p} requires a complexity of $\mathcal{O}(N_t^3)$. With the convergence accuracy ϵ , the overall complexity of Algorithm 2 is $\mathcal{O}(\log(\epsilon^{-1})N_t^3)$.

V. NUMERICAL RESULT

In this section, we illustrate the numerical results of the proposed Linear-Proximal algorithm. Three baseline algorithms

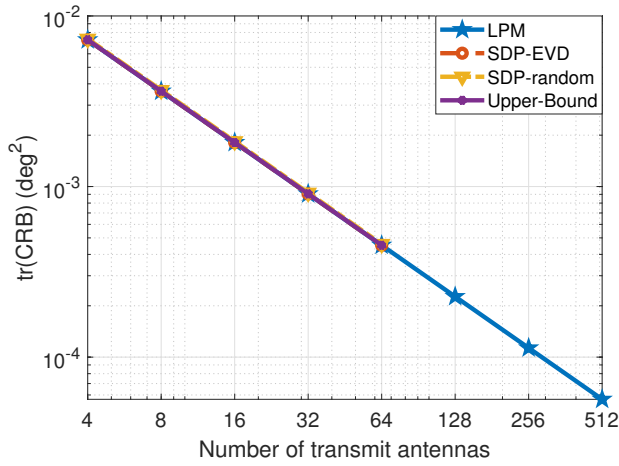


Fig. 1. CRB versus the number of transmit antennas when $P_t = 10$ dBm.

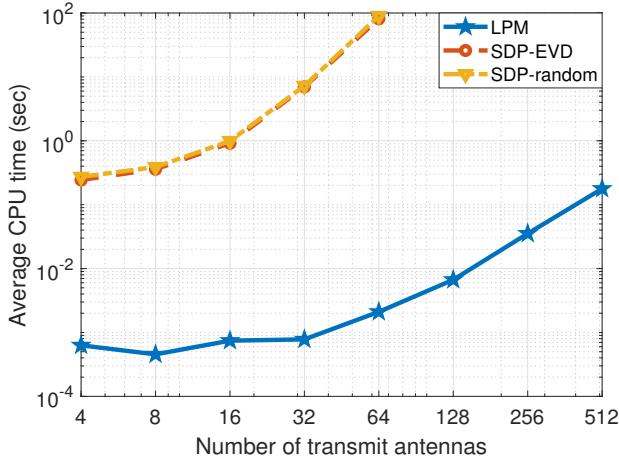


Fig. 2. CPU time versus the number of transmit antennas when $P_t = 10$ dBm.

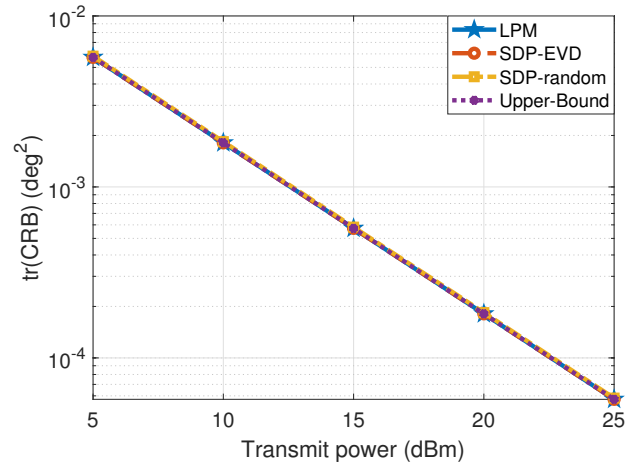


Fig. 3. CRB versus the transmit power when $N_t = 16$.

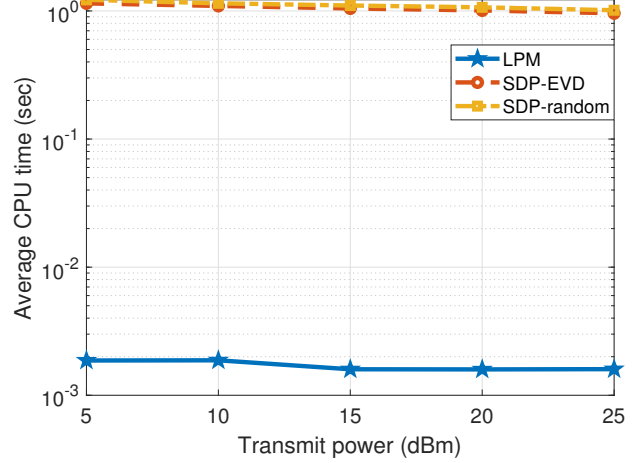


Fig. 4. CPU time versus the transmit power when $N_t = 16$.

are considered, as specified in Section III. The implementation of all the experiments relies on Windows 11 professional version, MATLAB 2022a and an Intel(R) Core(TM) i7-10700 CPU @ 2.90GHz processor. To mitigate the influence of chance and computer errors, all experimental results are averaged over 100 random trials.

Unless otherwise specified, we consider a MIMO radar with 9 receiver antennas ($N_r = 9$), the radar noise power is $\sigma_r^2 = 0$ dBm. The true target parameters are $\theta = 45^\circ$ with a velocity of $v = 8$ m/s. A total number of 1024 transmit symbols is considered within one CPI. The proposed algorithm is configured with a penalty coefficient of $\rho = 5$ and a convergence tolerance of $\epsilon = 10^{-5}$. The proposed algorithm initializes the transmit beamforming vector based on the direction of the transmission steering vector [29]. Following [5], the radar SNR is defined as $\frac{|\beta|^2 P_t}{\sigma_r^2} = 10$ dB, here $|\beta| = 1$.

The detection performance of the proposed algorithm and the baseline algorithms is depicted in Fig. 1. Due to the

complexity of CVX-based algorithms, we only illustrate their results in the range of 4 to 64 transmit antennas. Note that the Upper-Bound does not provide a solution for the transmit beamforming vector \mathbf{p} ; rather, it only yields the optimal covariance matrix $\mathbf{P} = \mathbf{p}\mathbf{p}^H$. Consequently, such method cannot directly address Problem (5). We only consider it as the performance upper bound. From Fig. 1, we observe that as the number of transmit antennas increases, the trace of the CRB for target estimation decreases for all algorithms. It is evident that the proposed LPM achieves the same performance as all other benchmark algorithms, including the Upper-Bound algorithm.

In Fig. 2, we illustrate the average CPU time consumption for all algorithms as the number of antennas increases. It should be noted that although Section IV-B indicates that the convergence rate of LPM is only sub-linear, the proposed LPM reduces the average CPU time by at least two orders of magnitude compared to the benchmark algorithms. Since the Upper-Bound algorithm cannot solve Problem (5), its CPU time is meaningless, and thus omitted from Fig. 2.

Fig. 3 illustrates the CRB performance for all algorithms, covering a range of the transmit power from 5 dBm to 25 dBm. As the transmit power increases, the CRB value decreases for all algorithms, indicating an enhancement of the target detection accuracy. Additionally, the performance of our proposed algorithm aligns with that of the baseline algorithms.

In Fig. 4, we present the average CPU time consumption for all algorithms as the transmit power increases. It is evident that our proposed algorithm significantly reduces the average CPU time compared to the baseline algorithms.

VI. CONCLUSION & OUTLOOK

In this paper, for designing waveform in MIMO radar systems, a novel low-complexity algorithm to solve non-convex SDP problem is proposed based on linear approximation and proximal term. As a theoretical contribution, we also prove the sub-linear convergence property of the proposed algorithms. Numerical results demonstrate that the proposed algorithm significantly reduces the CPU time while maintaining comparable performance. Future work includes exploring the potential applications of this algorithm in ISAC systems [30] and initialization-free variants of the proposed algorithm with faster convergence rate.

REFERENCES

- [1] M. Banafaa, I. Shaya, J. Din, M. Hadri Azmi, A. Alashbi, Y. Ibrahim Daradkeh, and A. Alhammedi, "6g mobile communication technology: Requirements, targets, applications, challenges, advantages, and opportunities," *ALEX ENG J.*, vol. 64, pp. 245–274, Feb. 2023.
- [2] X. Yu, K. Alhujaili, G. Cui, and V. Monga, "MIMO radar waveform design in the presence of multiple targets and practical constraints," *IEEE Trans. Signal Process.*, vol. 68, pp. 1974–1989, Mar. 2020.
- [3] G. Cui, H. Li, and M. Rangaswamy, "MIMO radar waveform design with constant modulus and similarity constraints," *IEEE Trans. Signal Process.*, vol. 62, no. 2, pp. 343–353, Jan. 2014.
- [4] X. Song, J. Xu, F. Liu, T. X. Han, and Y. C. Eldar, "Intelligent reflecting surface enabled sensing: Cramér-Rao bound optimization," *IEEE Trans. Signal Process.*, vol. 71, pp. 2011–2026, May. 2023.
- [5] L. Yin, Y. Mao, O. Dizdar, and B. Clerckx, "Rate-splitting multiple access for 6G—part II: Interplay with integrated sensing and communications," *IEEE Commun. Lett.*, vol. 26, no. 10, pp. 2237–2241, Jul. 2022.
- [6] F. Liu, Y. Cui, C. Masouros, J. Xu, T. X. Han, Y. C. Eldar, and S. Buzzi, "Integrated sensing and communications: Toward dual-functional wireless networks for 6G and beyond," *IEEE J. Sel. Areas Commun.*, vol. 40, no. 6, pp. 1728–1767, Mar. 2022.
- [7] H. Hua, J. Xu, and Y. C. Eldar, "Near-field 3D localization via MIMO radar: Cramér-Rao bound analysis and estimator design," *arXiv preprint arXiv:2308.16130*, 2023.
- [8] M. Xiong, J. Zhuo, Y. Dong, and X. Jing, "A layout strategy for distributed barrage jamming against underwater acoustic sensor networks," *J. Mar. Sci. Eng.*, vol. 8, no. 4, p. 252, Mar. 2020.
- [9] J. Li, L. Xu, P. Stoica, K. W. Forsythe, and D. W. Bliss, "Range compression and waveform optimization for MIMO radar: A Cramér-Rao bound based study," *IEEE Trans. Signal Process.*, vol. 56, no. 1, pp. 218–232, Jan. 2008.
- [10] F. Pukelsheim, *Optimal design of experiments*. SIAM, 2006.
- [11] S. Boyd and L. Vandenberghe, *Convex optimization*. Cambridge university press, 2004.
- [12] L. Yin and B. Clerckx, "Rate-splitting multiple access for dual-functional radar-communication satellite systems," in *Proc. IEEE Wireless Commun. Netw. Conf. (WCNC)*, Apr. 2022, pp. 1–6.
- [13] S. Boyd and L. Vandenberghe, "Semidefinite programming relaxations of non-convex problems in control and combinatorial optimization," in *Communications, Computation, Control, and Signal Processing: a tribute to Thomas Kailath*. Springer, 1997, pp. 279–287.
- [14] L. Vandenberghe and S. Boyd, "Semidefinite programming," *SIAM review*, vol. 38, no. 1, pp. 49–95, 1996.
- [15] A. Ben-Tal and A. Nemirovski, "Lectures on modern convex optimization 2020," *SIAM, Philadelphia*, 2021.
- [16] M. Grant and S. Boyd, "CVX: Matlab software for disciplined convex programming, version 2.1," <http://cvxr.com/cvx>, Mar. 2014.
- [17] Z.-Q. Luo, W.-K. Ma, A. M.-C. So, Y. Ye, and S. Zhang, "Semidefinite relaxation of quadratic optimization problems," *IEEE Signal Process. Mag.*, vol. 27, no. 3, pp. 20–34, May 2010.
- [18] F. Liu, Y.-F. Liu, A. Li, C. Masouros, and Y. C. Eldar, "Cramér-Rao bound optimization for joint radar-communication beamforming," *IEEE Trans. Signal Process.*, vol. 70, pp. 240–253, Dec. 2021.
- [19] R. M. Freund, "Introduction to semidefinite programming (SDP)," *Massachusetts Institute of Technology*, pp. 8–11, 2004.
- [20] H. Qi, X. Wu, and L. Jia, "Semidefinite programming for unified tdoa-based localization under unknown propagation speed," *IEEE Commun. Lett.*, vol. 24, no. 9, pp. 1971–1975, May. 2020.
- [21] O. Mehanna, N. D. Sidiropoulos, and G. B. Giannakis, "Joint multicast beamforming and antenna selection," *IEEE Trans. Signal Process.*, vol. 61, no. 10, pp. 2660–2674, Mar. 2013.
- [22] X. Du, A. Engelmann, T. Faulwasser, and B. Houska, "Approximations for optimal experimental design in power system parameter estimation," in *Proc. IEEE Conf. Decis. Control*, Jun. 2022, pp. 5692–5697.
- [23] N. Jorge and J. W. Stephen, *Numerical optimization*. Springer, 2006.
- [24] B. Lemaire, "The proximal algorithm," *International series of numerical mathematics*, vol. 87, pp. 73–87, 1989.
- [25] A. N. Iusem, "Augmented lagrangian methods and proximal point methods for convex optimization," *Investigación Operativa*, vol. 8, no. 11–49, p. 7, 1999.
- [26] Y. Nesterov *et al.*, *Lectures on convex optimization*. Springer, 2018, vol. 137.
- [27] L. Xu, J. Li, P. Stoica, K. W. Forsythe, and D. W. Bliss, "Waveform optimization for mimo radar: A cramer-rao bound based study," in *2007 IEEE International Conference on Acoustics, Speech and Signal Processing - ICASSP '07*, vol. 2, Apr. 2007, pp. II–917–II–920.
- [28] N. Sidiropoulos, T. Davidson, and Z.-Q. Luo, "Transmit beamforming for physical-layer multicasting," *IEEE Trans. Signal Process.*, vol. 54, no. 6, pp. 2239–2251, Jun. 2006.
- [29] T. Lo, "Maximum ratio transmission," in *1999 IEEE International Conference on Communications (Cat. No. 99CH36311)*, vol. 2, 1999, pp. 1310–1314 vol.2.
- [30] K. Chen, Y. Mao, L. Yin, C. Xu, and Y. Huang, "Rate-splitting multiple access for simultaneous multi-user communication and multi-target sensing," *IEEE Trans. Veh. Technol.*, pp. 1–6, Apr. 2024.